Formation and Detection of Solitonic Waves in Dilatant Granular Materials: Potential Application for Nonlinear NDT

Martin LINTS[1], Andrus SALUPERE[1], Serge DOS SANTOS[2]

1 Institute of Cybernetics at Tallinn University of Technology, martin.lints@cens.ioc.ee, salupere@ioc.ee
2 INSA Centre Val de Loire, U930 Inserm-Université de Tours, F-41034 Blois, France, serge.dossantos@univ-tours.fr

Abstract
In this paper, wave propagation in dilatant granular material, modelled with the hierarchical Korteweg–de Vries equation, is simulated numerically using a cnoidal initial wave. It is found that the balance between micro- and macrostructure determines the number of solitons emerging from the input. Results can be applied in nonlinear NDT for determination of material parameters. Additionally, the formation of hidden solitons [1] which affect the solution is analysed. It is found that when the spatial period of the input wave is short compared to material length, the hidden solitons form and can be detected from their effect on visible solitons and in case of harmonic input, with methods of Discrete Spectral Analysis [2]. This would require consideration in theoretical and practical treatises.

Keywords: Solitons, microstructure, dilatant granular materials, nonlinear elasticity

1 Introduction

Recent ten years have seen considerable development of optimized signal processing methods for improving nonlinear NDT methods derived from Nonlinear Elastic Wave Spectroscopy (NEWS). Using symmetry invariance and Time Reversal (TR), the classical NEWS methods are supplemented and improved by new excitations having the intrinsic property of enlarging time-frequency scales. This is the case of TR-NEWS, now recognized as a useful tool for microcracks detection of various complex samples [3], but also for nonlinear scatterers localization in the wide sense [4]. TR-NEWS signal processing is performed using symmetrisation of coded-excitation practically realized using pulse-inversion methods. Response to positive and negative excitations allows the extraction of nonlinear signature of the sample under test. Among these family of "pulse coded excitation", solitonic coding constitutes a new scheme in the sense that solitons are the best candidates for pulse propagation in nonlinear and dispersive media. Their robustness during propagation could inform aeronautic end-users during monitoring process of layered; granular, lightweight or functionally graded materials. One of the main advantages of this approach is the possibility of taking into account intrinsic space scales, namely, the size of the grains or the distance between microcracks. It has been proved [5] that in such a medium dispersion and nonlinearity could be combined in the way that solitonic propagation could be observed experimentally [6].

2 Dilatant granular materials

Granular materials are complex environment for the propagation of waves due to the heterogeneity caused by the micro- and the macrostructure. The effect of the microstructure has been widely attributed to cause the emergence of solitons [7, 8]. The nonlinearities arise due to geometrical effects and in cohesionless materials, the lack of the rarefaction wave.

Tightly packed granular material is dilatant if the voidage expands upon deformation [9]. For an example, in an idealised case of a bed of spherical granular material, the bed must expand under shearing motion, increasing its void volume [10], one such example being packed sand in a watery environment. A possible model for the wave motion in such a material was derived by Giovine and Oliveri [11] under somewhat restrictive assumptions:

- The case is conservative.
- The particles are elastic.
- The particles are surrounded by compressible fluid.
- Fluid density is negligible compared to density of particles.
- In a ball of radius ζ are no diffusion of grains nor any relative rotations (of grain, etc.).

The resulting equation governs the nonlinear wave motion near the equilibrium in dilatant granular materials:

$$\frac{\partial u}{\partial t} + u\frac{\partial u}{\partial x} + \alpha_1 \frac{\partial^3 u}{\partial x^3} + \beta \frac{\partial^2}{\partial x^2}\left(\frac{\partial u}{\partial t} + u\frac{\partial u}{\partial x} + \alpha_2 \frac{\partial^3 u}{\partial x^3}\right) = 0, \tag{1}$$

where

u is	bulk density,
x is	space coordinate,
t is	time coordinate,
α_1 is	macrostructure dispersion parameter,
α_2 is	microstructure dispersion parameter,
β is	microstructure parameter describing the ratio of grain size and wavelength.

The sign of β depends on the ratio of kinetic and potential energies and is positive for lower values of kinetic energy and negative with higher values [12].

3 Numerical Analysis

Equation (1) can only be solved numerically, in this paper by a simple and very broadly applicable pseudospectral method by first using Fast Fourier Transform to calculate the spatial derivatives and then advancing the solution in time using a ordinary differential equation (ODE) solver. The spatial derivatives are found by differentiating the spectrum of trigonometric functions and taking the inverse transform. The equation is solved [2] by rewriting Eq. (1):

$$(u + \beta u_{xx})_t + (u + 3\beta u_{xx})\, u_x + (\alpha_1 + \beta u)\, u_{3x} + \beta\alpha_2 u_{5x} = 0$$

where variable $\phi = u + \beta u_{xx}$ is substituted in, expressing the time derivative

$$\phi_t = -(u + 3\beta u_{xx})\, u_x - (\alpha_1 + \beta u)\, u_{3x} - \alpha_2 \beta u_{5x}$$

This equation can be integrated with ODE solvers if the variable u and its derivatives are expressed by

$$u = \mathrm{F}^{-1}\left[\frac{\mathrm{F}\phi}{1-\beta k^2}\right], \qquad \frac{\partial^n u}{\partial x^n} = \mathrm{F}^{-1}\left[\frac{(ik)^n \mathrm{F}\phi}{1-\beta k^2}\right].$$

getting the requirement for the value of β that $1 - \beta k^2 \neq 0$.

The initial conditions (ICs) considered here are firstly the cnoidal wave, given by

$$u(x) = A \cdot \mathrm{cn}^2\left[x\sqrt{\frac{A-\eta}{12\cdot\alpha_1}},\ \sqrt{m}\right], \tag{2}$$

where A is the amplitude and m is the elliptic parameter [13], K is Legendre's complete elliptic integral of the first kind. Period is chosen $P = 2\pi$ and η, which unites the shape of the profile and the period, is obtained from

$$P = 4 \cdot \sqrt{\frac{3\alpha_1}{A-\eta}} \cdot K(\sqrt{m}). \tag{3}$$

Secondly, the Eq. (1) is solved with "lengthened" cn^2 shaped IC:

$$u(x) = \begin{cases} 0 & , \quad 0 \leq x < 3\pi \\ A \cdot \mathrm{cn}^2\left[x\sqrt{\frac{A-\eta}{12\cdot\alpha_1}},\ \sqrt{m}\right] & , \quad 3\pi \leq x < 5\pi \\ 0 & , \quad 5\pi \leq x < 8\pi \end{cases} \tag{4}$$

Thirdly is used the sech^2-shaped input which is a single bell-shaped hump with $P = 8\pi$:

$$u(x) = A \cdot \mathrm{sech}^2\left[x\sqrt{\frac{A}{12\cdot\alpha_1}}\right]. \tag{5}$$

As the cnoidal wave is $P = 2\pi$ long, it is expected to yield more hidden solitons while "lengthened" cn^2 and sech^2-shaped are expected to show those solitons as visible. While the $P = 2\pi$ cnoidal wave and $P = 8\pi$ sech^2-shaped wave are analytical solutions to the macrostructural KdV part of HKdV in Eq. (1), the lengthened cn^2 is not. These three initial conditions are shown in Fig. 1 for various values of elliptic parameter m.

4 Parameter spaces

Numerical scanning of parameter spaces show what results could be expected in physical experiments. Previously, Ilison [12] has analysed the parameter space of HKdV (1) with $P = 16\pi$ sech^2 input and demonstrated that: for $\beta \leq 0.1111$, the number of emerging solitons is always one when $\alpha_1 > \alpha_2$; if $\beta \geq 1.111$ and again $\alpha_1 > \alpha_2$, the number of solitons increases with the ratio α_1/α_2 increasing; generally, a tail of oscillations will also be generated besides the solitons; in cases where $\alpha_1 < \alpha_2$, the wave profile will consist mostly of one hump and the tail; in the limiting case where α_1 is much smaller than α_2, the hump will disappear in the forming wave packet; HKdV where $\alpha_1 = \alpha_2$ leads to ordinary KdV and can be used for checking purposes.

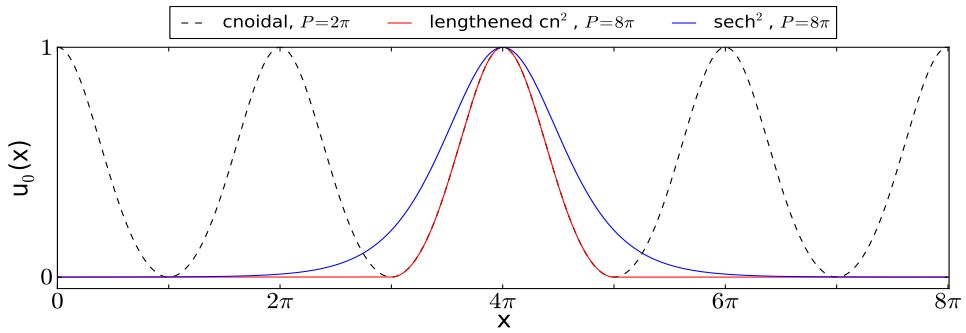

(a) ICs for $m = 0.5628$

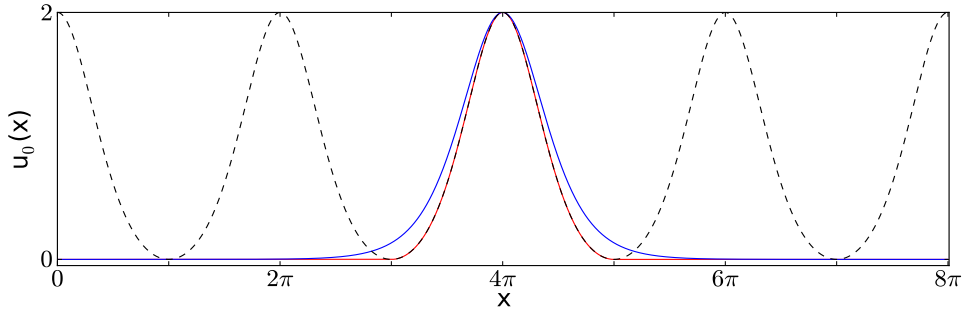

(b) ICs for $m = 0.8027$

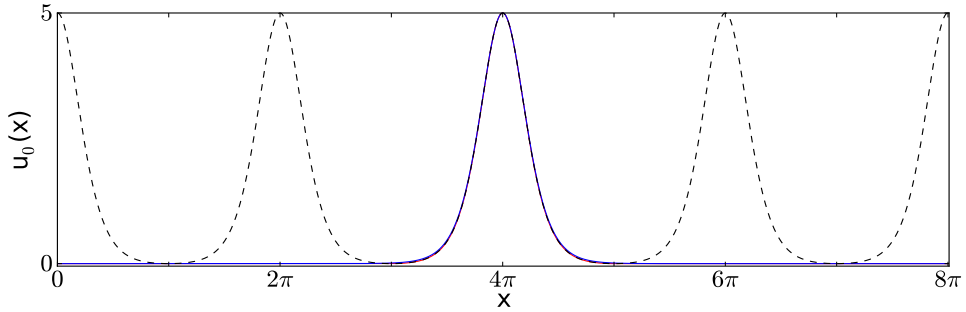

(c) ICs for $m = 0.9905$

Figure 1: Initial conditions

In this work, Ilison's results were corroborated and additionally found that there exist ratios α_1/α_2 where the solution is relatively free of the tail and generates a certain number of solitons (Fig. 2). This is probably due to some agreement between micro- and macrostructure at those specific parameter values. Solitons are in this paper defined as stable waves which interact elastically and do not lose amplitude, and propagate with a constant speed and amplitude. These α_1/α_2 ratios were better distinguished with $\beta = 111.11$ than $\beta = 11.111$. It turns out that with $\beta = const$, the nature of the solution depends entirely on the shape of the input (in case of cnoidal wave, the elliptic parameter m) and the ratio of dispersion parameters α_1/α_2. In the present study, it has been found that the elliptic parameter of the cnoidal-based ICs used can be kept constant with the relation

$$m \sim \frac{A}{\alpha_1}\left(\frac{P}{\pi}\right)^2 . \tag{6}$$

Upon fixing the m and α_1/α_2, the results are practically the same within a type of IC (Fig. 3). Table 1 shows in columns *No. sol.-s* the number of visible solitons plus hidden in parentheses. The wave amplitudes and propagation times can be normalised by IC amplitudes, resulting identical solutions with waves coinciding completely at all times (Fig. 4). Increasing the α_1/α_2

ratio increases the number of visible and hidden solitons formed. In the future analysis, the amplitude A and period P of the cnoidal wave and macrostructural dispersion parameter α_1 can be dropped from the parameter space and only two values: the shape of the initial wave and the ratio of the dispersion parameters.

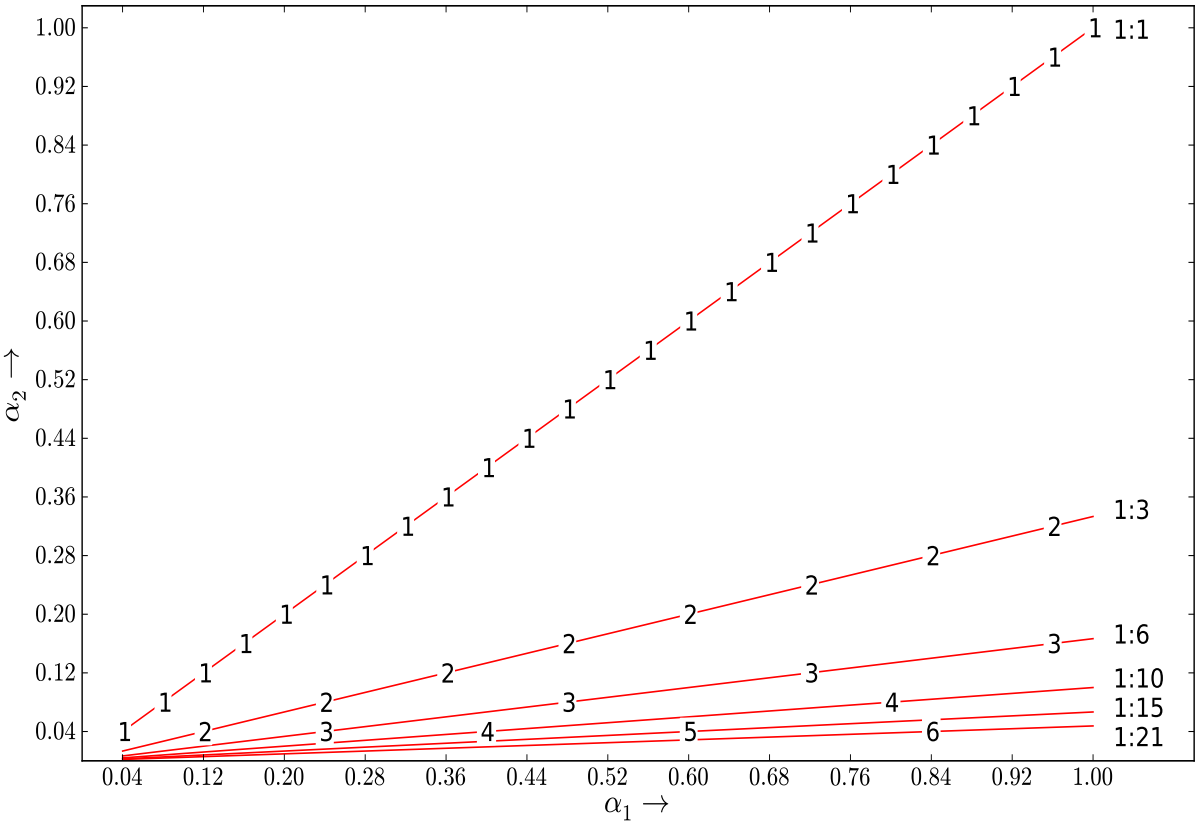

Figure 2: Number of emerging solitons against parameters α_1 and α_2 ($N = 1024$, $P = 16\pi$, $\beta = 111.11$, $A = 5.0$, sech^2 initial profile)

5 Hidden solitons

Hidden solitons are important for nondestructive testing applications, because they can cause changes in visible solitons (specific to soliton-type interaction) and can be amplified in non-conservative cases and carry substantial energy [1]. In practical applications they could form in cases where the material thickness is small compared to the wavelength. Hidden solitons are those which do not emerge before the interactions begin (due to short spatial period) [14]. The number of hidden solitons generally depends on the period length and the total number of emerging solitons. These control whether the soliton train can fully emerge before the interactions begin. These hidden solitons affect the visible ones via the interactions.

The pseudocolor plot (with nonlinear colormap to distinguish the low-amplitude waves) of the solutions shows the emerging wave trajectories and mostly visible solitons. Then, the small-amplitude and hidden solitons are recognized from the maxima curves plot [14], which traces the evolution of the maxima of the solution. The maxima curves exhibit a concavity or a local minimum where the soliton interacts with a smaller one. As the model equation and initial waves analysed here are quite general, the interaction concavities remain the most important

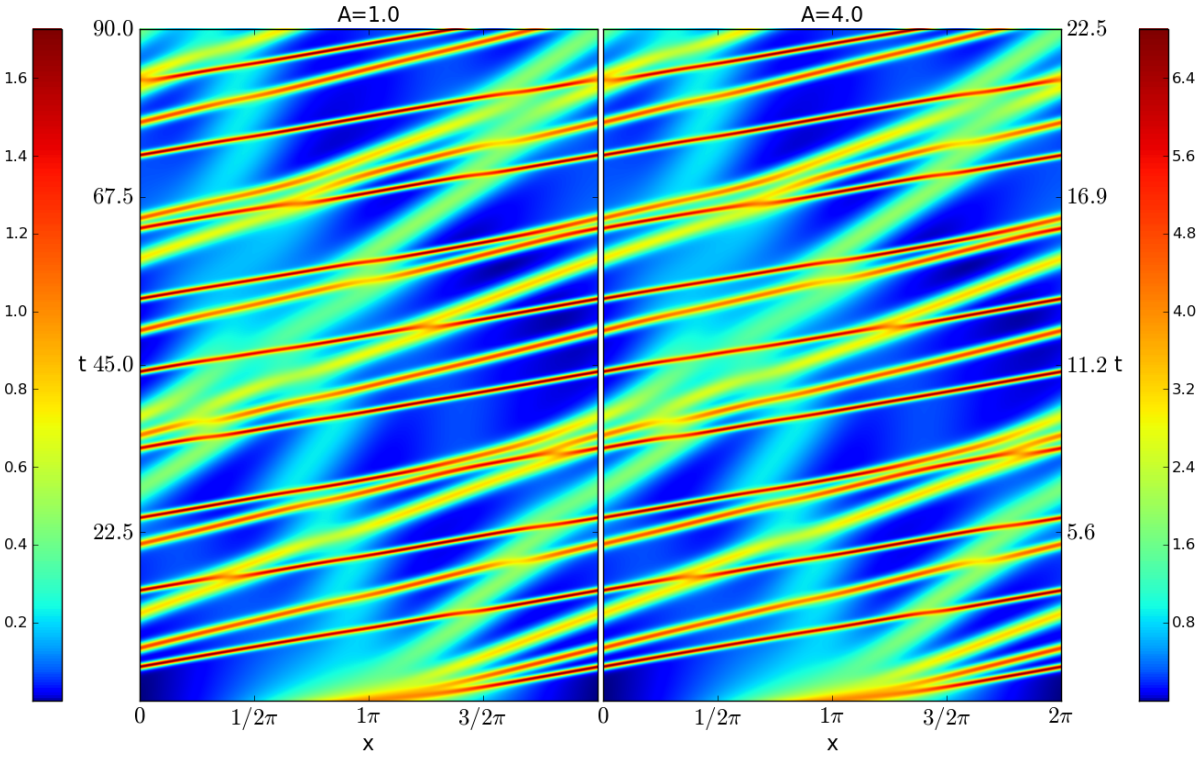

Figure 3: Pseudocolor plots ($m = 0.9530$, $\alpha_1/\alpha_2 = 25$)

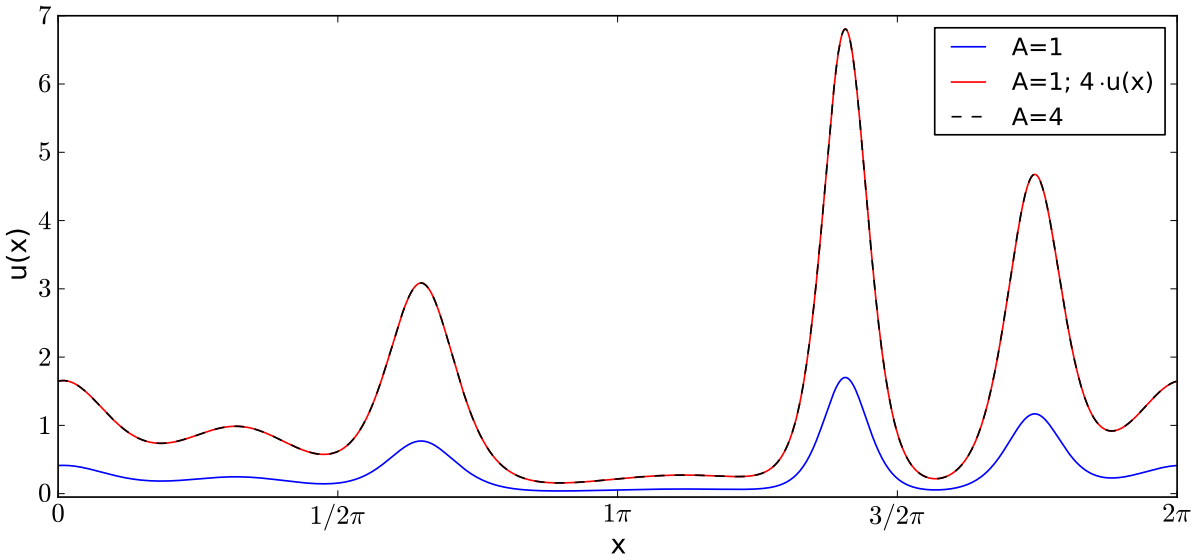

Figure 4: Final profiles of Fig. 3

Table 1: Results where $m = 0.9530$, showing visible solitons plus hidden solitons in parentheses

A	α_1	$\frac{\alpha_1}{\alpha_2}$	α_2	cnoidal, $P = 2\pi$	"length." cn^2, $P = 8\pi$	sech^2, $P = 8\pi$
				No. sol.-s	No. sol.-s	No. sol.-s
4.0	0.4	72.7	0.00550	8(+2)	10+tail	10(+1)
		25.0	0.01600	5(+1)	6+tail	6(+1)
		14.3	0.02800	4(+1)	5+tail	5
3.0	0.3	72.7	0.00413	8(+2)	10+tail	10(+1)
		25.0	0.01200	5(+1)	6+tail	6(+1)
		14.3	0.02100	4(+1)	5+tail	5
1.0	0.1	72.7	0.00138	8(+2)	10+tail	10(+1)
		25.0	0.00400	5(+1)	6+tail	6(+1)
		14.3	0.00700	4(+1)	5+tail	5

method for detecting the hidden solitons. Any changes in the visible solitons amplitudes must correspond to either the evolution of the initial wave into separate solitons or the interaction between various solitons, including visible and hidden solitons. This is the most robust way of detecting an interaction with a hidden soliton.

To analyse the solution further, the spectral amplitudes (SA) of the DSA [2] may be used. It is possible to synthesise the waveform using cosine series

$$u(x,t) = a_0(t) + \sum_{k=1}^{N/2} a_k(t)\cos[kx + \phi_k(t)].$$

Here the quantities $a_k(t)$

$$\begin{aligned} a_0(t) &= \frac{U(0,t)}{N}, \\ a_k(t) &= \frac{2|U(k,t)|}{N}, \qquad k = 1, 2, \ldots, \frac{N}{2} - 1, \\ a_k(t) &= \frac{|U(k,t)|}{N}, \qquad k = \frac{N}{2}, \end{aligned}$$

are called *spectral amplitudes* and $\phi_k(t)$ is the *phase spectrum*.

Every interaction between solitons is reflected by a local minimum or concavity in the higher soliton's maxima curve. *Spectral amplitude* curves can be used to find the total number of solitons (including the hidden ones) of KdV solution from the harmonic input [2]. The time moments t_k are introduced, where t_1 stands for the time of the first spectral recurrence and the time moments t_k ($k > 1$) correspond to the maximum value of the k-th spectral amplitude a_k in the time interval $0 < t < t_{k-1}$ (as a rule these maxima are global in $0 < t < t_1$). In that case: if the time of the first maximum of the k-th spectral curve is denoted as t_k, then the first

and k-th soliton interact for the first time near time moment t_{k-1} and second and k-th near time moment t_{k-2} and so on. Having determined the total number of solitons, the hidden ones are those which remain hidden in the *initial* soliton train [14]. Spectral methods allowed to detect the interactions of solitons in cases where the initial wave is close to harmonic (cnoidal wave with $m < 0.6$).

As hoped, the cnoidal initial wave with its short, $P = 2\pi$ period allows to generate solutions where the emerging solitons start interacting before the train is fully formed, generating hidden solitons (Table 1). Furthermore, the corresponding lengthened cn^2-shaped input generates comparable number of solitons which are all usually visible. Unfortunately, cnoidal and "lengthened" cn^2-shaped inputs do not generally generate identical total number of solitons, so lengthening the period does not give any more information and every shape of the initial wave must be considered separately. Nevertheless, the hidden solitons remain an important concept in theory and practical experiments, because they can emerge irrespective of the initial condition used and carry enough energy to visibly affect the solution.

6 Conclusions

If the dilatant granular material can be modelled by Eq. (1) (for example 1D materials such as layered composites), it has been found that the cnoidal input is highly suitable for analysing the material microstructure and the properties of the solution, as the cnoidal wave can be chosen to agree with the macrostructure. Furthermore, the number of emerging solitons depend on the ratio of micro- and macrostructural dispersion ratios. This could be used in experiments for determining the material parameters. Additionally, future simulations can be simplified by dropping the explicit amplitude A period length P and macrostructural dispersion parameter α_1 from the parameter space and replacing it with the shape m of cnoidal wave and ratio α_1/α_2.

The cnoidal input also allows to analyse what happens if the material length is small, compared to the wavelength. This is simulated by choosing a small period ($P = 2\pi$) for the cnoidal wave. The results indicate that hidden solitons could be formed in case of high ratio α_1/α_2 (generating large number of solitons), when the interactions begin before smaller solitons are fully formed. This shows that hidden solitons, which can contain energy, can affect the solution visibly.

References

[1] J. Engelbrecht, A. Salupere, On the problem of periodicity and hidden solitons for the KdV model, Chaos 15 (2005) 015114.

[2] A. Salupere, The pseudospectral method and discrete spectral analysis, in: E. Quak, T. Soomere (Eds.), Applied Wave Mathematics: Selected Topics in Solids, Fluids, and Mathematical Methods, Springer, Berlin, 2009, pp. 301–333.

[3] S. Dos Santos, Z. Prevorovsky, Imaging of human tooth using ultrasound based chirp-coded nonlinear time reversal acoustics, Ultrasonics 51 (6) (2011) 667–674.

[4] M. Frazier, B. Taddese, T. Antonsen, S. M. Anlage, Nonlinear time reversal in a wave chaotic system, Phys. Rev. Letters 110.

[5] L. Ilison, A. Salupere, P. Peterson, On the propagation of localised perturbations in media with microstructure, Proc. Estonian Acad. Sci. Phys. Math. 56 (2) (2007) 84–92.

[6] A. M. Lomonosov, V. V. Kozhushko, P. Hess, Laser-based nonlinear surface acoustic waves: from solitary to bondbreaking shock waves, Proc 18th International Symposium on Nonlinear Acoustics ISNA. Americal Institute of Physics (2008) 481–490.

[7] A. M. Samsonov, G. V. Dreiden, I. V. Semenova, On the existence of bulk solitary waves in plexiglas, Proc. Estonian Acad. Sci. Phys. Math. 52 (1) (2003) 115–124.

[8] S. R. Hostler, Wave propagation in granular materials, Ph.D. thesis, California Institute of Technology (2005).

[9] O. Reynolds, Experiments showing dilatancy, a property of granular material, possibly connected with gravitation, in: Papers on Mechanical and Physical Subjects, Vol. 2, Cambridge University Press, 1901, pp. 217–227.

[10] M. Massoudi, M. M. Mehrabadi, A continuum model for granular materials: Considerding dilatancy and the Mohr–Couloumb criterion, Acta Mechanica 152 (2001) 121–138.

[11] P. Giovine, F. Oliveri, Dynamics and Wave Propagation in Dilatant Granular Materials, Meccanica 30 (4) (1995) 341–357.

[12] L. Ilison, Solitons and solitary waves in hierarchical Korteweg–de Vries type systems, Ph.D. thesis, Tallinn University of Technology (2009).

[13] G. A. Korn, T. M. Korn, Mathematical handbook for scientists and engineers, Dover publications, Inc., 2000.

[14] A. Salupere, G. A. Maugin, J. Engelbrecht, Korteweg–de Vries soliton detection from a harmonic input, Phys. Lett. A 192 (1) (1994) 5–8.